TECHNICAL UNIVERSITY OF CLUJ-NAPOCA

ACTA TECHNICA NAPOCENSIS

Series: Applied Mathematics, Mechanics, and Engineering
Vol. 69, Issue I, March, 2026

STRESS CONDITIONS IN IMPROVED CUTTER TEETH DESIGNED FOR THE BUCKET WHEELS OF EXCAVATORS WORKING IN OPEN PITS

Alin Daniel RADU, Gheorghe-Bogdan URDEA

Abstract: *This paper presents the results of research on the design of a range of standard-sized teeth with improved characteristics for excavators working in coal mines, based on the specific cutting resistance of coal and rock in open pits. The results are based on experimental tests conducted in laboratory conditions involving the cutting of coal and rock samples taken from representative mining fields of S.N.L. Oltenia.*
Key words: *bucket wheel excavators, cutting resistance, stress condition analysis, Von Mises theory*

1. INTRODUCTION

Following experimental tests of shear displacement of coal and rock from the Oltenia mining basin, on samples taken from different mining fields, the tangential, normal, and lateral forces were measured and recorded on a set of standard teeth mounted on a shear device using a strain gauge dynamometer.

By processing the recorded data, the range of variation of the specific cutting resistances of coal and rock was obtained, after which the maximum forces on the teeth of the bucket
.
wheel of excavators working in different quarries were determined. Knowing the forces that load the cutting teeth, three types of teeth were designed, with improved characteristics compared to those used so far, for three distinct ranges of specific cutting resistance.

2. RESULTS OBTAINED

Table 1 shows the geometric parameters of the three tooth sizes.

Table 1

The geometric parameters of the three tooth sizes

No.	Geometric parameters (Symbol)	Tooth size		
		I	II	III
1	Clearance angle (α)	52°	47°	55°
2.	Angle of inclination (β)	7°	7°	7°
3.	Sharpening angle (δ)	31°	36°	31°
4.	Cutting angle (γ)	38°	43°	35°
5.	Longitudinal lateral angle (ξ)	5°	5°	5°
6.	Transverse lateral angle (θ)	3°	3°	3°
7.	Width of the cutting edge of the tooth (b)	120 mm	120 mm	120 mm
8.	Angle of inclination of the seating surface (φ)	13°	15°	13°

Figure 1 shows how the tooth is attached to the bucket wheel of the excavator.

Figure 2 shows the shape and geometric characteristics of the tooth for sizes I and II. These tooth sizes have the same shape but differ in their geometric parameters and active part. Type I has a larger clearance angle, a smaller sharpening angle, and is intended for cutting

Received: 30.01.26; **Similarities**: 17.02.26: **Reviewed**: 23.02. /26.02.26: **Accepted** 23.03.26.

lignite with a lower specific cutting resistance (*A = 400...800 N/cm*), such as that found in the Jilţ, Roşia, and Husnicioara quarries. Type II has a smaller clearance angle, a larger sharpening angle and is recommended for cutting lignite with higher specific resistance (A = 800...1200 N/cm), found in the Olteţu and Peşteana quarries.

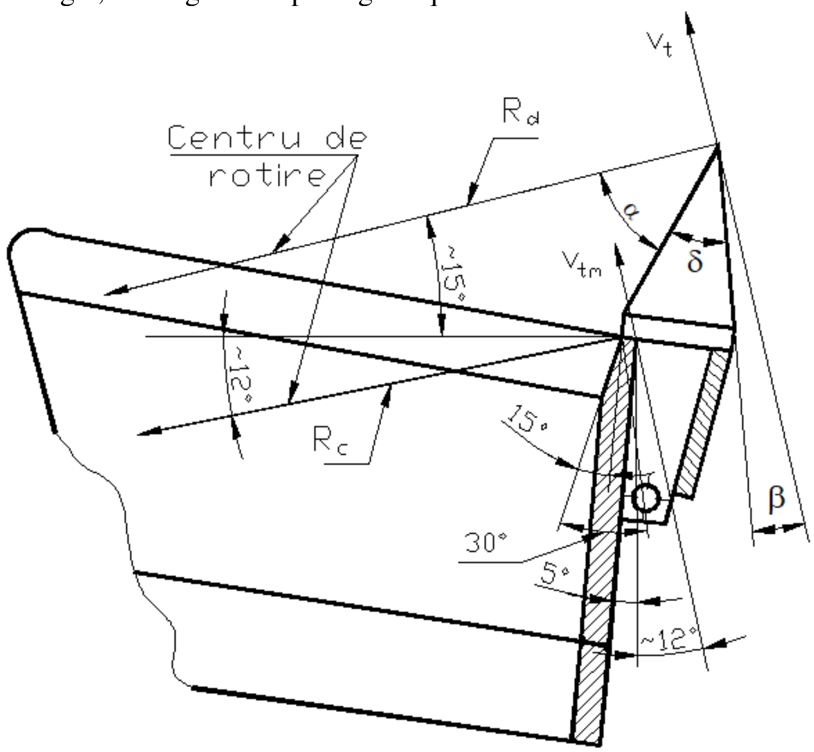

Fig.1. Tooth mounting diagram on the cup

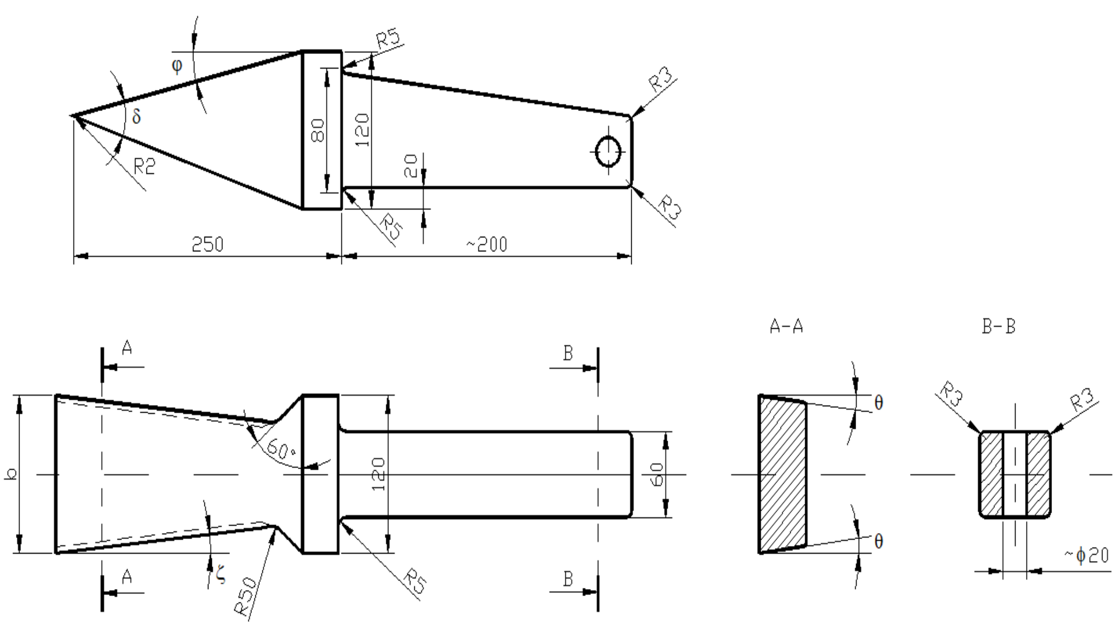

Fig.2. Sketch and geometric parameters for type I and II teeth

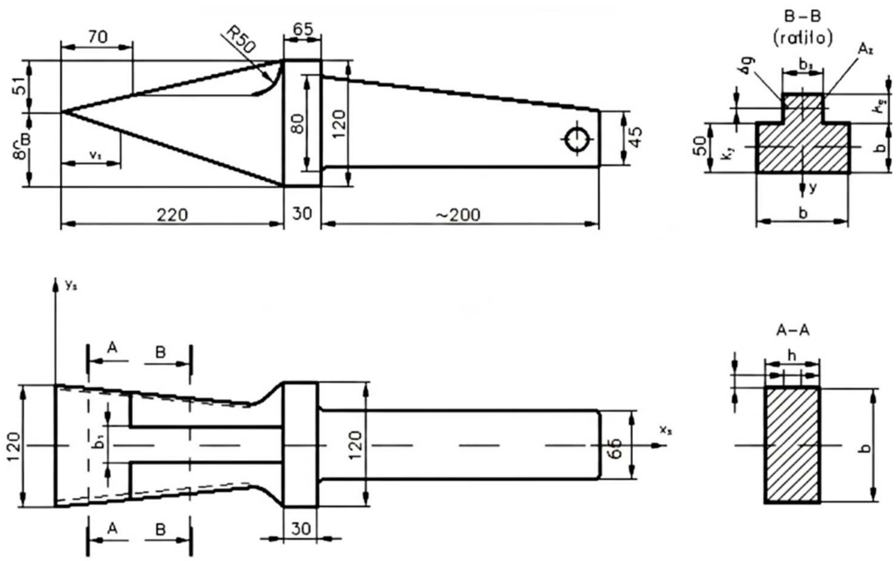

Fig.3. Sketch and geometric characteristics of the type III tooth

Figure 3 shows the shape and geometric characteristics of the type III tooth, which can cover the entire range of specific cutting resistances.

18 kN, and $F_z= 10\ kN$. The decomposition of these forces in relation to the tooth results in:

$$F_{y1}=F_x \cos 52^o - F_y \cos 38^o = 2,275 \cdot 10^4 N;$$
$$F_{x1}=F_x \sin 52^o - F_y \sin 38^o = 5,87 \cdot 10^4 N;$$
$$F_{z1}=10 \cdot 10^4 N.$$

These forces were used to determine the stress state in type III, which has a more flexible construction.

These forces represent the results of specific loads that are randomly distributed on the active faces of the tooth, and in a covering calculation, they were considered to be applied to the tip of the tooth.

The proposed material for the teeth is 41MoCr11, or equivalent, with $\sigma_{02}=750\ N/mm^2$, $\sigma_r=950\ N/mm^2$, which is a medium-hardness alloy steel recommended for heat-treated parts. The expression of the maximum stress in a current section of the tooth in the range $y_1 \in [0;70]$ mm, from both axial and bending stress, is:

$$\sigma = -10^4 \left(\frac{5,836}{65,448 x_1 - 0,0934 x_1^2} + \frac{2,275 x_1}{5,949 x_1^2 - 0,00866 x_1^3} + \frac{10^4}{1308 x_1 - 3,799 x_1^2 - 0,00276 x_1^3} \right) \quad (1)$$

where x_1 is entered in mm and the stress is obtained in N/mm^2 .

Figure 4 shows the stress variation graph over the interval $x = 0...70\ mm$, at the most stressed points of the active part of the tooth, from which it follows that high stress values are achieved near the cutting edge.

This is because in the calculation, the tooth was hypothetically considered to have a sharp tip, but in reality the tip is rounded with a radius of *2.5 mm*.

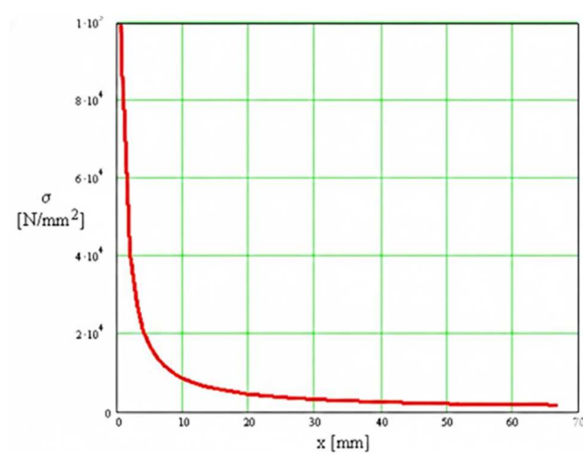

Fig.4 Graph showing the variation of maximum stress over the interval $x \in [0;70]\ mm$

The complex shape of the tooth cross-section over the interval $x_1 \in [70...220]$ *mm* required the determination of stress at the most stressed points for different values of the abscissa x_1, resulting in the graph of maximum stress variation over this interval shown in Figure 5. The maximum stress values at the most stressed points of this interval were obtained using the following relationship:

$$\sigma = -10^4 \left(\frac{5,837}{A} + \frac{5,836 \cdot e}{W_{z1}} + \frac{2,275 \cdot x_1}{W_{z1}} + \frac{x_1}{W_{y1}} \right)$$

where A, $W_{(z1)}$, and W_{y1} are the area and resistance modules at the points considered, and e is the eccentricity of force F_{x1} relative to the center of the sections.

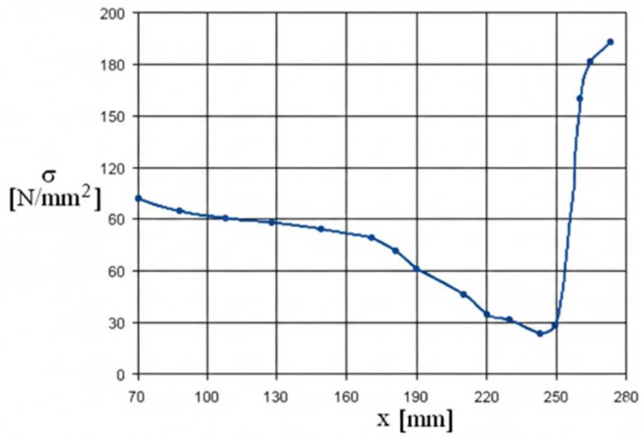

Fig.5 Graph of maximum stress variation over the interval $x \in [70; 275]$ *mm*

Figure 5 also shows the variation of the stress over the interval $x = 220...250$ *mm*, over the interval $x = 220...230$ *mm* of the active part with a square section of 120×120 mm^2 and, respectively, on the tooth tail up to the section embedded in the tooth (interval $x = 250...275$ *mm*), on which the section was considered constant and rectangular with dimensions 66×66.5 mm^2.

The jump in stress from 28.39 N/mm^2 to 162.43 N/mm^2 in the $x = 250$ *mm* section is due to the jump in tooth section from the active part to the tooth root (which is fixed in the cup). In the section where the tooth dimensions vary abruptly, a stress concentration factor of $\beta_k \approx 2$ is achieved, resulting in a maximum stress of σ_{max} N/mm^2 and a safety factor of $c = 2.3$ in this section

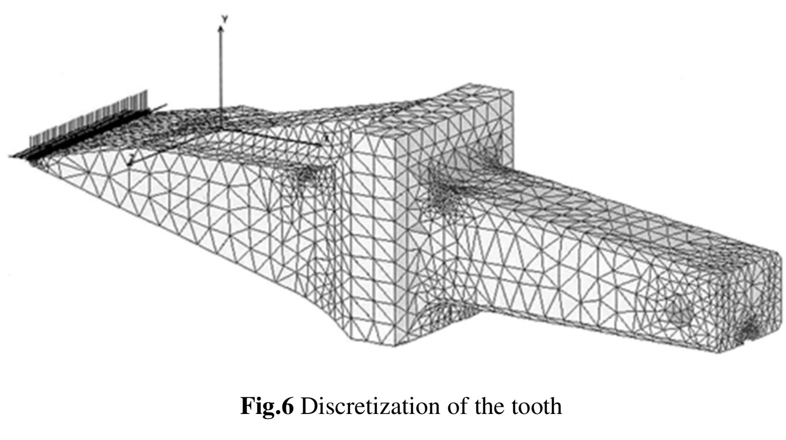

Fig.6 Discretization of the tooth

The stress state in the tooth was also determined using the finite element method. Figure 6 shows the discretization of the tooth, and Figure 7 shows the stress state, where the stresses are given in daN/cm^2.Figure 7 shows that at the most stressed points, in the area of section variation, stresses of 300 N/mm^2 are achieved, compared to 324 N/mm^2 obtained by classical calculation.

Figure 8 shows the tooth studied in a 3D representation created using the SOLID EDGE program.

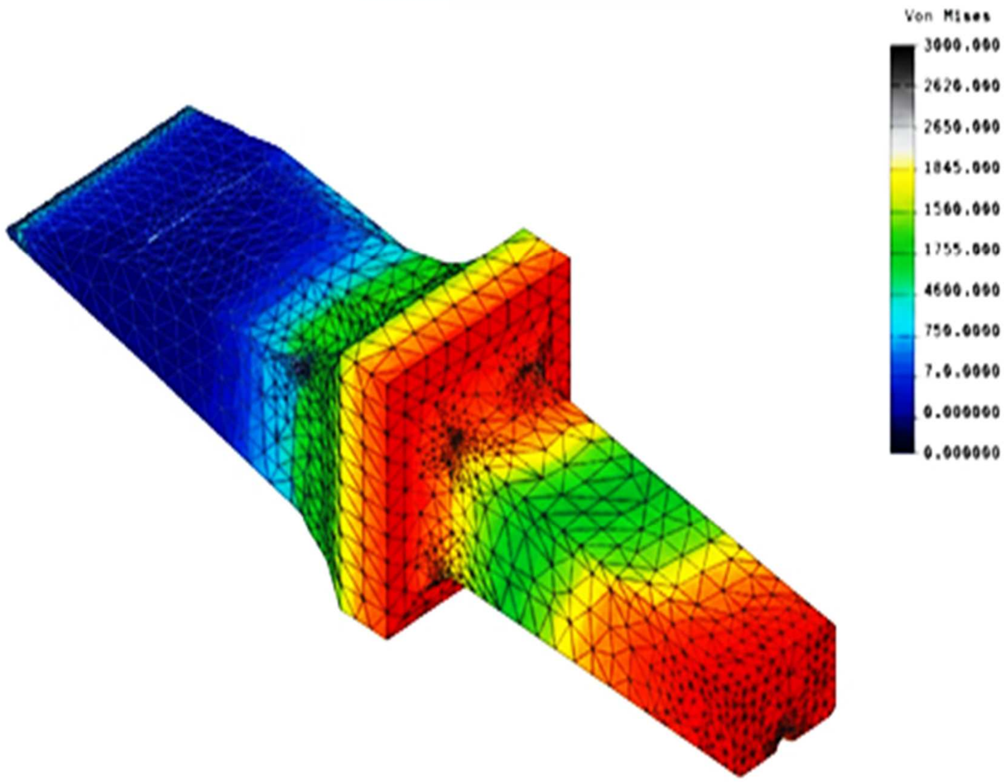

Fig.7 Stress state according to Von Mises theory

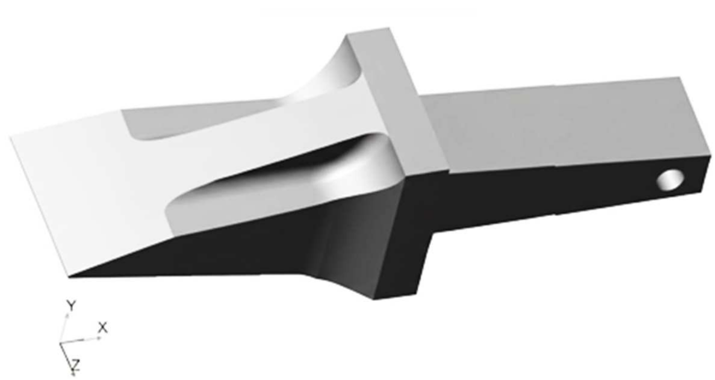

Fig.8 The structural shape of the tooth

3. CONCLUSIONS

Experimental laboratory research, followed by analyses and studies, has made it possible to establish the geometric parameters for the three types of tooth sizes, which work advantageously in the dislocation of lignite and rock from the surface.

The next stage of research is to determine the location of the teeth on the buckets and their direction, as well as to establish the optimal material from which they should be made and the treatments necessary to achieve maximum wear resistance.

The experimental tests to be carried out under real conditions will allow these problems to be solved and the research to be completed, which could lead to significant savings in the mining industry.

4. REFERENCES

[1] Kunze, G. et al. Baumaschinen – Erdbau- und Tagebaumaschinen. Springer

Vieweg, Berlin, 2012.
[2] Sadowski, T.; Marsavina, L. Dynamic hardness testing methods and applications in engineering materials. Journal of Materials Testing, 2016; 58(7): 623–633.; [9] Sant'Anna, A.; Pereira, T. Predictive maintenance using hardness-based structural integrity indicators in mining components. International Journal of Mining Science and Technology, 2019; 29: 891–899.
[3] Bathe, K. J., Finite Element Procedures, Prentice Hall, New Jersey, SUA, 1996.
[4] Cook, R. D., Malkus, D. S., Plesha, M. E., Witt, R. J., Concepts and Applications of Finite Element Analysis, 4th Edition, John Wiley & Sons, New York, SUA, 2002.
[5] Dassault Systèmes, Abaqus 2025 Documentation – Theory Guide, Dassault Systèmes Simulia Corp., Providence, Rhode Island, SUA, 2025.
[6] Dassault Systèmes, Abaqus 2025 Documentation – Scripting User's Guide, Dassault Systèmes Simulia Corp., Providence, Rhode Island, SUA, 2025.
[7] Gautam Puri,Python Scripts for ABAQUS, ISBN: 978-0-615-52050-6 , 2011
[8] McKyes, E., Soil Cutting and Tillage, Elsevier, Amsterdam, Olanda, 1985.
[9] Boresi, A. P., Schmidt, R. J., Sidebottom, O. M. Advanced Mechanics of Materials 6th Edition, Wiley, 2003

STAREA DE TENSIUNI ÎN DESIGNUL ÎMBUNĂTĂȚIT AL DINȚILOR DE TĂIERE DESTINAȚI ROȚILOR PORT-CUPE ALE EXCAVATOARELOR CARE LUCREAZĂ ÎN CARIERE

Rezumat: Această lucrare prezintă rezultatele cercetărilor privind proiectarea unei game de dinți de dimensiuni standard cu caracteristici îmbunătățite pentru excavatoarele care lucrează în minele de cărbune, pe baza rezistenței specifice la tăiere a cărbunelui și a rocii în carierele deschise. Rezultatele se bazează pe teste experimentale efectuate în condiții de laborator, implicând tăierea probelor de cărbune și rocă prelevate din bazine miniere reprezentative ale S.N.L. Oltenia.

Alin Daniel RADU, Lecturer, University of Petroșani, Department of Mechanical, Industrial and Transport Engineering, alinradu@upet.ro, 20 Universității str., +40 254 542580

Gheorghe-Bogdan URDEA, Lecturer, University of Petroșani, Department of Mechanical, Industrial and Transport Engineering, gheorgheurdea@upet.ro, 20 Universității str., +40 254 542580